

# Articles

## The Determination of Interconversion Barriers of Oxygen-Containing Cyclohexene Analogues

Jaebum Choo\*, Soo-No Lee<sup>†</sup>, and Kuk-Haeng Lee<sup>‡</sup>

\*Department of Chemistry, Hanyang University, 396 Daehak-dong, Ansan 425-791, Korea

<sup>†</sup>Department of Chemistry, Texas A&M University, College Station, TX 77843, USA

<sup>‡</sup>Department of Chemical Education, Chonbuk National University, Chonju 560-756, Korea

Received May 20, 1995

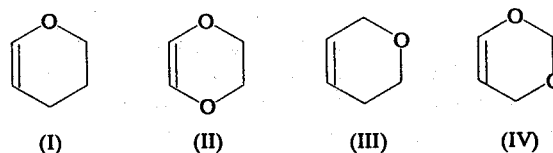
The interconversion barriers between two twisted conformers of four oxygen-containing cyclohexene analogues have been investigated utilizing a periodic hindered pseudorotational model, molecular mechanics (MM3) calculations, and previously reported far-infrared spectra. The six-fold pseudorotational potential energy function satisfactorily fits the observed bending transitions. The interconversion barrier heights calculated from the pseudorotational model show excellent agreement with those determined from two-dimensional potential energy surfaces for the ring-bending and ring-twisting vibrations. The barriers to interconversion range from  $3350\text{ cm}^{-1}$  (9.6 kcal/mol) to  $3890\text{ cm}^{-1}$  (11.1 kcal/mol) for four oxygen-containing cyclohexene analogues.

### Introduction

Six-membered ring compounds are major building blocks of nature's organic and bioorganic systems. Thus, it is very important to analyze the conformational structures and dynamics of these ring systems because the interconversion barriers to conformational changes and the lowest energy pathway play an important role in chemical activities and kinetics. Conformational preferences and interconversion barriers between conformers can be determined by understanding the nature of potential energy surfaces as a function of the nuclear coordinates. Both computational and experimental methods have been utilized to determine the molecular potential energy surfaces.<sup>1,2</sup> *Ab initio*, Molecular Mechanics, and semi-empirical MO calculations are the well-known computational techniques. On the other hands, FT-IR, laser-induced Raman, NMR, microwave, electron diffraction, and laser-induced fluorescence are most widely used spectroscopic techniques to determine the potential energy functions of ring systems. Especially, vibrational spectroscopy using infrared and Raman instrumentation has been a powerful tool to study the conformational structure and molecular dynamics of small ring systems over the last two decades.<sup>3-5</sup> With the improvements of high resolution capability in FT-IR and laser technology in Raman instrumentation, quantum mechanical methods to determine the potential energy functions from vibrational data have been extensively developed together.<sup>6-8</sup>

Recently, there have been numerous studies of the large amplitude out-of-plane vibrations of small ring molecules because these vibrations contain a large amount of information of molecular conformations and interatomic forces.<sup>9-13</sup> The illumination of out-of-plane ring vibrations are very important for several reasons. First, the out-of-plane motions are

the vibrational modes to determine the ring skeletons. Second, they occur in the low frequency region ( $10\text{-}400\text{ cm}^{-1}$ ) of the vibrational spectra and can be isolated from high frequency modes. Third, a large number of quantum states are populated and the vibrational transitions originating from vibrational excited states can be observed. Thus, far-infrared or low frequency Raman gas phase spectroscopic data can be used to determine accurate potential energy surfaces for out-of-plane vibrations of ring compounds.



A six-membered ring with a double bond has two low frequency out-of-plane vibrational modes because the C=C double bond restrains one of the out-of-plane modes (ring-twisting about the double bond) and increases its vibrational frequency. The other two low-frequency modes (ring-bending and single bond ring-twisting) appear in the far-infrared region ( $<400\text{ cm}^{-1}$ ) and they are coupled together if they are close in the frequency. Oxygen-containing cyclohexene analogues such as 3,4-dihydro-2H-pyran(I), 2,3-dihydro-1,4-dioxin(II), 5,6-dihydro-2H-pyran(III), and 4H-1,3-dioxin(IV) have been widely investigated utilizing microwave spectra, far-infrared spectra, and molecular mechanics(MM2) calculations. Lord, Rounds, and Ueda<sup>14</sup> analyzed the far-infrared spectra of 3,4-dihydro-2H-pyran(I) and 2,3-dihydro-1,4-dioxin(II) and used the data to define a two-dimensional potential energy surface in terms of the ring-bending and ring-twisting coordinates. Wells *et al.*<sup>15</sup> and Lopez *et al.*<sup>16</sup> studied the molecular structures using microwave spectra of these compounds. Allinger *et al.*<sup>17</sup> and Anet *et al.*<sup>18</sup> determined the equilibrium structure and interconversion barriers using MM2 calcula-

\*To whom correspondence should be addressed.

tions. Dixon *et al.*<sup>19</sup> determined one-dimensional ring-twisting potential energy functions of 5,6-dihydro-2H-pyran(III) and 4H-1,3-dioxin(IV) from their far-infrared spectra. More recently, Tecklenburg and Laane introduced the kinetic energy expansion functions of asymmetric six-membered rings using bond vector models.<sup>20</sup> They determined more reliable two-dimensional potential energy surfaces for these ring systems including the kinetic expansion functions to the vibrational Hamiltonian and by choosing more reasonable basis sets at the twisting potential energy minima.<sup>21</sup> However, the interconversion barriers, which represents the energies required for the lowest energy form to a second equivalent form, determined by the far-infrared and the molecular mechanics methods show different values to each other. In light of the discrepancies, we reinvestigated these molecules utilizing pseudorotational potential model. In this model the interconversion process between two twisted conformations through a bent form is treated as a periodic hindered pseudorotation. The pseudorotational study of cyclohexene has previously been reported.<sup>12</sup> In this study, the interconversion barrier was estimated to be 8.4-12.1 kcal/mol range from the vibrational data and the pseudorotational model. This range was higher than the values of MM3 or *ab initio* but it was compatible with the far-infrared and NMR results. In the present study, we extend our studies to four oxygen-containing cyclohexene analogues by examining the previously reported far-infrared spectra and by determining one-dimensional pseudorotational potential energy functions of these molecules. The results provide the application possibility of one-dimensional pseudorotational model and the quantitative picture of the conformational processes for the asymmetric six-membered rings.

## Theory and Calculations

### Pseudorotational Potential Energy Calculations.

Oxygen-containing cyclohexene analogues can be considered as pseudo-heterocyclic five membered rings because the olefinic carbon atoms are locked together and move as a single unit during the vibrational motions. Thus these compounds can be considered as the pseudo-five-membered rings. In the pseudorotation process, the ring interconverts between two twisted forms. The phase angle of pseudorotation  $\phi$  and the radial coordinate  $r$ , which are related to the ring bending and ring-twisting coordinates in Figure 1, can be used to represent the pseudorotation and radial motions. The one-dimensional vibrational Hamiltonian for the hindered pseudorotation can be expressed by

$$H_{\phi} = -B \frac{d^2}{d\phi^2} + \sum_{n=0}^6 \frac{V_n}{2} (1 - \cos n\phi) \quad (1)$$

where  $\phi$  is the phase angle of pseudorotation and the potential energy constants  $V_n$  for  $n=2, 4$  and  $6$  have been used.<sup>24</sup> The pseudorotational constants  $B$  is given by

$$B = \frac{\hbar^2}{2} \left( \frac{1}{\mu r^2} \right) \quad (2)$$

where  $\mu$  is the reduced mass of the ring compound and  $\mu r^2$  is the moment of inertia which is dependent on the radial coordinate  $r$ . For a free pseudorotor, the energy can be expressed by

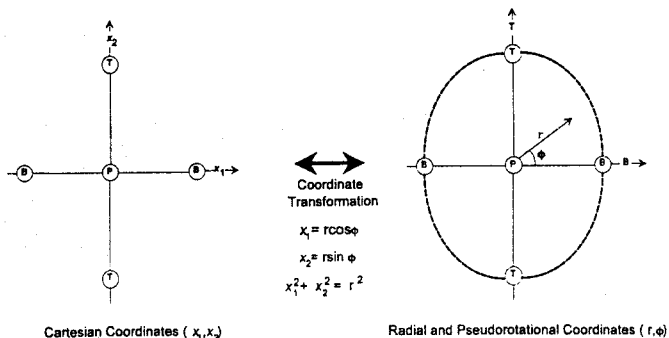


**Figure 1.** Coordinate transformation between polar( $r, \phi$ ) and Cartesian( $x_1, x_2$ ) coordinates for the out-of-plane vibrations of ring compounds.

$$E_{\phi} = n_{\phi}^2 B \quad n_{\phi} = 0, \pm 1, \pm 2, \dots \quad (3)$$

where  $n_{\phi}$  is the origin of the vibrational transition.

The two-dimensional Cartesian coordinate potential energy functions of oxygen-containing cyclohexene analogues in terms of ring-bending( $x_1$ ) and ring-twisting( $x_2$ ) coordinates can be transformed to the polar coordinate potential energy functions in terms of radial( $r$ ) and pseudorotational( $\phi$ ) coordinates.<sup>12,23</sup> Figure 1 shows the coordinate transformation between Cartesian ( $x_1, x_2$ ) and polar ( $r, \phi$ ) coordinates. T is the lowest energy twist form and B is the intermediate energy bend form. P is the highest energy planar form when both bending and twisting coordinates are zero. The dot line in Figure 1 shows the interconversion process between bending and twisting conformers. In this process, the potential energy function can be expressed as the function of radial( $r$ ) and pseudorotational ( $\phi$ ) coordinates. Here it is assumed that the variables  $r$  and  $\phi$  can be separated because the radial band appears at higher frequency region than the pseudorotational band. Thus, one-dimensional pseudorotational potential energy function is utilized to calculate the vibrational energy levels and interconversion barriers. The pseudorotational function at a fixed radial distance  $r=r_0$  is usually truncated after the 6th term and given by

$$V(\phi) = \frac{1}{2} V_2 (1 - \cos 2\phi) + \frac{1}{2} V_4 (1 - \cos 4\phi) + \frac{1}{2} V_6 (1 - \cos 6\phi) \quad (4)$$

where  $V_2$  represents the interconversion barrier to pseudorotation while  $V_4$  and  $V_6$  help to adjust the potential shape. The odd-powered terms can typically be neglected because of symmetry rule.  $\phi$  represents pure twisting vibration when  $\phi=0, \pi, 2\pi$ , pure bending vibration when  $\phi=\pi/2, 3\pi/2$ , and the vibration including both bending and twisting when  $0 < \phi < \pi/2, \pi/2 < \phi < \pi \dots$ .

The vibrational Hamiltonian in equation (1) is used to calculate the vibrational energy levels. The Hamiltonian can be set up in exponential terms and this is transformed to symmetry adapted sin-cos basis sets using Wang transformation.<sup>7</sup> The program was written by Laane *et al.*<sup>24</sup> Seventy basis functions are used for both even and odd symmetry blocks and the least square iteration method is used to fit the observed frequencies.

**Molecular Mechanics (MM3) Calculations.** Molecular mechanics (MM3) is the computational method to determine the conformational structure and minimum energy of

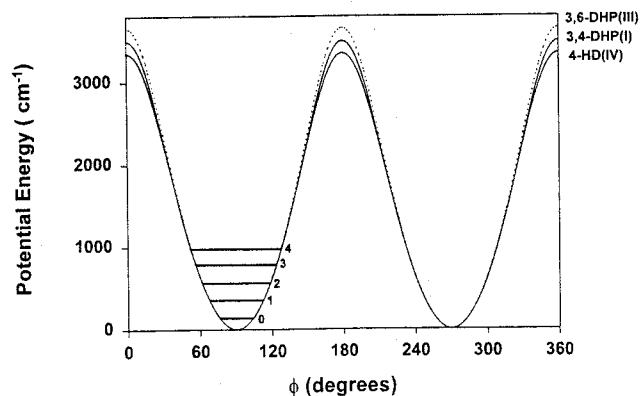
**Table 1.** Observed and Calculated Vibrational Frequencies ( $\text{cm}^{-1}$ ) for Various Potential Energy Functions for 3,4-Dihydro-2H-pyran(I), 5,6-Dihydro-2H-pyran(III), and 4H-1,3-Dioxin(IV)

Transition	Observed <sup>a</sup>	Calculated	
		2D Cartesian $V_{246}$	Pseudorotation
<b>3,4-Dihydro-2H-pyran(I)</b>			
0 $\rightarrow$ 1	177.2	175.1 <sup>b</sup>	177.3 <sup>c</sup>
1 $\rightarrow$ 2	175.8	174.7	175.7
2 $\rightarrow$ 3	174.5	174.2	174.5
3 $\rightarrow$ 4	173.4	173.7	173.5
4 $\rightarrow$ 5	172.5	173.1	172.6
5 $\rightarrow$ 6	172.0	172.5	171.9
<b>5,6-Dihydro-2H-pyran(III)</b>			
0 $\rightarrow$ 1	177.3	172.9 <sup>c</sup>	177.3 <sup>c</sup>
1 $\rightarrow$ 2	175.5	173.8	175.6
2 $\rightarrow$ 3	174.4	174.3	174.3
3 $\rightarrow$ 4	173.4	174.5	173.4
4 $\rightarrow$ 5	172.7	174.6	172.6
5 $\rightarrow$ 6	172.0	174.6	172.1
<b>4H-1,3-Dioxin(IV)</b>			
0 $\rightarrow$ 1	189.6	187.5 <sup>d</sup>	189.2 <sup>e</sup>
1 $\rightarrow$ 2	188.5	188.7	188.5
2 $\rightarrow$ 3	187.0	189.0	187.7
3 $\rightarrow$ 4	187.0	189.0	186.8

<sup>a</sup> refs. 6 and 11. <sup>b</sup> ref. 12;  $V(x_1, x_2) = 4.24 \times 10^5 x_1^4 - 1.01 \times 10^4 x_1^2 + 2.48 \times 10^4 x_2^4 - 2.01 \times 10^4 x_2^2 + 1.70 \times 10^5 x_1^2 x_2^2$ . <sup>c</sup> ref. 12;  $V(x_1, x_2) = 5.99 \times 10^5 x_1^4 - 1.19 \times 10^4 x_1^2 + 2.09 \times 10^4 x_2^4 - 1.86 \times 10^4 x_2^2 + 1.74 \times 10^5 x_1^2 x_2^2$ . <sup>d</sup> ref. 12;  $V(x_1, x_2) = 7.08 \times 10^5 x_1^4 - 1.04 \times 10^4 x_1^2 + 3.08 \times 10^4 x_2^4 - 2.08 \times 10^4 x_2^2 + 2.27 \times 10^5 x_1^2 x_2^2$ . <sup>e</sup>  $V = 3443/2(1 + \cos 2\phi) + 395/2(1 + \cos 4\phi) + 56/2(1 + \cos 6\phi)$ ;  $B = 3.4 \text{ cm}^{-1}$ . <sup>f</sup>  $V = 3592/2(1 + \cos 2\phi) + 433/2(1 + \cos 4\phi) + 64/2(1 + \cos 6\phi)$ ;  $B = 3.3 \text{ cm}^{-1}$ . <sup>g</sup>  $V = 3323/2(1 + \cos 2\phi) + 312/2(1 + \cos 4\phi) + 27/2(1 + \cos 6\phi)$ ;  $B = 3.9 \text{ cm}^{-1}$ .

a molecule using empirically determined force constants and structural parameters in the program.<sup>25</sup> The calculated total steric energy consists of several components based on the intramolecular interactions such as compression energy, angle-bending energy, torsional energy, dipole energy, stretch-bend energy, and van der waals energy. In the energy minimization process, it is possible to restrict the motions of selected atoms or the plane of symmetry to obtain the desired conformational structure. The lowest energy of a out-of-plane conformer can be calculated without any restriction. The energy of a planar conformer can be calculated by fixing the  $z$  coordinates of all of the ring atoms.

The molecular mechanics methods are very useful for several purposes. First, they can be used to estimate the interconversion barriers to planarity and pseudorotation for ring molecules. Second, the total steric energy as a function of vibrational coordinate can be calculated and this energy can be directly compared to the experimental potential energy function. Third, molecular mechanics can calculate vibrational frequencies using Wilson's harmonic approximation and these calculated frequencies can be compared to the observed frequency values. The force constant parameters of the newer MM3 program are quite different and more reliable than those of MM2.

**Figure 2.** Pseudorotational potential energy curves for 3,4-dihydro-2H-pyran(I), 5,6-dihydro-2H-pyran(III), and 4H-1,3-dioxin(IV).

## Results and Discussion

Table 1 lists the observed vibrational frequencies reported by Lord *et al.*<sup>14</sup> and Dixon *et al.*<sup>19</sup> The calculated frequencies from the two-dimensional potential energy surfaces and the pseudorotational models are also listed. In the pseudorotational potential energy calculations, the best fits with the observed frequencies were obtained when pseudorotational constant  $B = 3.4 \text{ cm}^{-1}$  and interconversion barrier (the energy difference between the twisted and bent conformers)  $B_{int} = 3500 \text{ cm}^{-1}$  (10.0 kcal/mol) for 3,4-DHP(I),  $B = 3.3 \text{ cm}^{-1}$  and  $B_{int} = 3660 \text{ cm}^{-1}$  (10.5 kcal/mol) for 5,6-DHP(III),  $B = 3.9 \text{ cm}^{-1}$  and  $B_{int} = 3550 \text{ cm}^{-1}$  (9.6 kcal/mol) for 4-HD(IV), respectively. In the cases of 5,6-DHP(III) and 4-HD(IV), the vibrational frequencies calculated from two-dimensional energy surfaces show increasing anharmonic trends with the increase of vibrational quantum number while those calculated from the pseudorotational functions show decreasing anharmonic trends. In addition, the frequencies calculated from the pseudorotational functions almost perfectly match with the observed values. For the oxygen-containing cyclohexene analogues(I, III, and IV), the pseudorotational parameters to determine the potential functions are in very close ranges ( $B(3.4\text{--}3.9 \text{ cm}^{-1})$ ,  $V_2(3323\text{--}3592 \text{ cm}^{-1})$ ,  $V_4(312\text{--}433 \text{ cm}^{-1})$ , and  $V_6(27\text{--}64 \text{ cm}^{-1})$ ) because the pseudorotational bands of the compounds are observed in the similar frequency regions of far-infrared spectra. Their pseudorotational potential functions are plotted in Figure 2. The potential function shows the maximum (bending structure) when  $\phi = 0^\circ$ ,  $180^\circ$ , and  $360^\circ$  while it shows the minimum (twisting structure) when  $\phi = 90^\circ$  and  $270^\circ$ . The intermediate values correspond to the interconversion structures between the ring-bending and ring-twisting.

2,3-DD(II) has  $C_{2v}$  symmetry when the ring is planar. The lowest energy conformation of this ring is half-chair (twist,  $C_2$  symmetry) and the interconversion process occurs from one twist form to another *via* boat (bend,  $C_s$  symmetry) form. The MM3 energy calculations for the bending and twisting motions are available using  $C_2$  symmetry axis. Figure 3 shows the pseudorotational potential function (solid line), MM3 potential function (dot line), the observed transitions, and the pseudorotational quantum states for the molecule. The observed and calculated frequencies (two-dimensional Cartesian model, MM3, and six-fold pseudorotational model) are compared in Table 2. The anharmonicity predicted by MM3

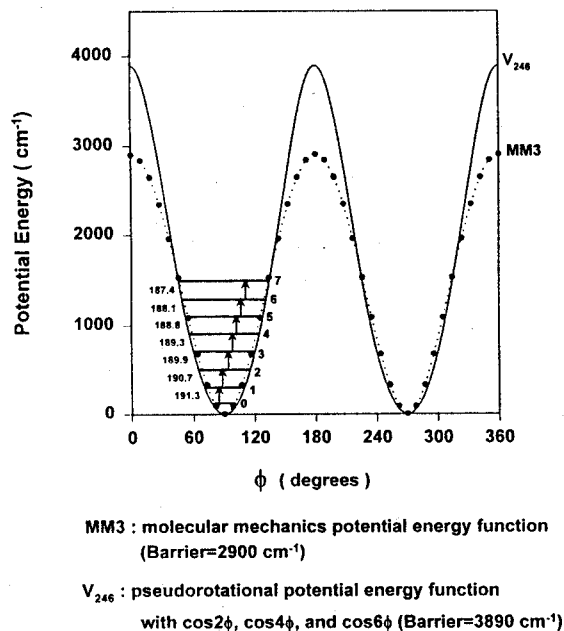


**Figure 3.** Pseudorotational potential energy curves and observed vibrational transitions of 2,3-dihydro-1,4-dioxin(II).

**Table 2.** Observed and Calculated Vibrational Frequencies (cm<sup>-1</sup>) for Various Potential Energy Functions for 2,3-Dihydro-1,4-dioxin (II)

Transition	Observed <sup>a</sup>	Calculated		
		2D <sup>b</sup> Cartesian	V <sub>2</sub> <sup>c</sup> (MM3)	V <sub>246</sub> <sup>d</sup> (Pseudorot.)
0→1	191.3	190.6	191.4	191.4
1→2	190.7	190.5	188.0	190.6
2→3	189.9	190.2	184.5	190.0
3→4	189.3	189.9	180.9	189.3
4→5	188.8	189.5	177.1	188.8
5→6	188.1	189.0	173.3	188.2
6→7	187.4	188.4	169.3	187.4
Barrier (cm <sup>-1</sup> )		3830	2900	3890

<sup>a</sup> ref. 6. <sup>b</sup> ref. 12;  $V(x_1, x_2) = 1.59 \times 10^5 x_1^4 - 1.39 \times 10^4 x_1^2 + 2.92 \times 10^4 x_2^4 - 2.20 \times 10^4 x_2^2 + 1.96 \times 10^5 x_1^2 x_2^2$ . <sup>c</sup>  $V = 2900/2(1 + \cos 2\phi)$ ;  $B = 3.27$  cm<sup>-1</sup>. <sup>d</sup>  $V = 3848/2(1 + \cos 2\phi) + 421/2(1 + \cos 4\phi) + 46/2(1 + \cos 6\phi)$ ;  $B = 3.60$  cm<sup>-1</sup>.

is much less than the observed one. (the observed: 191.3(0-1) and 187.4(6-7), V<sub>2</sub>(MM3): 191.4(0-1) and 169.3(6-7)) On the other hand, the anharmonicities predicted by 2D Cartesian model and pseudorotational model show very good agreement with the observed anharmonicity. The interconversion barrier heights by three different methods are also listed in Table 2 and their potential functions are plotted in Figure 3. As shown in this figure, MM3 calculation greatly underestimates the interconversion barrier heights and this means that the actual potential well is considerably different from that predicted by MM3. The MM3 underestimation of barrier heights was reported by Choo *et al.*<sup>26</sup> Oxygen-containing ring molecules have larger C=C-O-C torsional constants,

**Table 3.** Interconversion Barriers (cm<sup>-1</sup>) and Energy Differences (cm<sup>-1</sup>) between the twisted and Planar Conformations

Molecule	2D Cartesian <sup>a</sup>		MM3 <sup>b</sup>		Pseudorotation <sup>c</sup>
	$\Delta E_{pt}$ <sup>d</sup>	$B_{int}$ <sup>e</sup>	$\Delta E_{pt}$	$B_{int}$	$B_{int}$
CH <sub>2</sub> CH <sub>2</sub> CH=CHOCH <sub>2</sub> (I)	4080	3480	3320	3130	3500
CH <sub>2</sub> OCH=CHOCH <sub>2</sub> (II)	4130	3830	2900	2900	3890
CH <sub>2</sub> CH <sub>2</sub> CH=CHCH <sub>2</sub> O(III)	4130	3540	3910	2520	3660
CH <sub>2</sub> OCH=CHCH <sub>2</sub> O(IV)	3500	3120	4410	3880	3350

<sup>a</sup> ref. 12. <sup>b</sup> molecular mechanics(MM3) calculation. <sup>c</sup> pseudorotational potential energy function model  $V = 1/2 \sum V_n (1 + \cos n\phi)$ . <sup>d</sup> the energy barrier between planar and twisted structures. <sup>e</sup> the energy barrier to interconversion,  $B_{int} = B_{pt} - B_{pb}$ .

due to the  $\pi$  interactions, than in the MM3 parametrization. When the second-fold torsional barrier term V<sub>2</sub> is increased to be 13.5 kcal/mol from 2.3 kcal/mol in MM3 program, the barrier height is about 3900 cm<sup>-1</sup> and this may be caused by the interactions between carbon-carbon  $\pi$  systems and the oxygen non-bonded p orbitals.

Table 3 compares the interconversion barriers of four cyclohexene analogues by three different calculational methods. What is evident from this table is that most of the ring molecules are oscillating in the bottom of the twisting potential wells which has the lowest energy and they are converted to another minimum through bending saddle points. The interconversion barrier heights calculated from the pseudorotational model show good agreement with those determined from two-dimensional potential energy surfaces<sup>21</sup> for the ring-bending and ring-twisting vibrations. The MM3 interconversion barriers which we have calculated here are somewhat lower (400-1000 cm<sup>-1</sup>) than those experimentally determined for four cyclohexene analogues. Plausible adjustment of the torsional MM3 Parameter leads to the good agreements between the calculated and experimental values.

## Conclusions

In this work we have tried to apply the pseudorotational potential model for five-membered rings to asymmetric six-membered rings. In this process these molecules have been assumed as the hindered pseudorotors. The barriers to interconversion from the far-infrared data and pseudorotational potential model range from 3350 cm<sup>-1</sup> (9.6 kcal/mol) to 3890 cm<sup>-1</sup> (11.1 kcal/mol) for four oxygen-containing cyclohexene analogues. These barrier heights show good agreement with the values (3120 cm<sup>-1</sup>-3830 cm<sup>-1</sup>) from the two-dimensional potential energy surface for the ring-bending and ring-twisting vibrations. Thus, we conclude that the pseudorotational fitting model, together with the low-frequency vibrational data, is a very useful method to determine the out-of-plane potential energy function and interconversion barriers for cyclohexene-like six-membered rings as well as for five-membered rings. When these results were viewed with the molecular mechanics and Microwave results, they provide a coherent picture of the conformational energy pathway between

the lowest energy conformers.

**Acknowledgment.** We are very grateful to Professor J. Laane at Texas A&M University for his support and encouragement.

### References

- Case, D. A. *Conformational Analysis of Medium-Sized Heterocycles*; Glass, R. S. Ed; VCH: New York, 1988.
- Fuchs, B. *Topics in Stereochemistry*; Volume 10; Eliel, E. L. & Allinger, N. L. Ed; John Wiley & Sons: New York, 1978.
- Laane, J. *Pure Appl. Chem.* **1987**, *59*, 1307.
- Legon, A. C. *Chem. Rev.* **1980**, *80*, 231.
- Laane, J. *Annu. Rev. Phys. Chem.* **1994**, *45*, 179.
- Malloy, T. B., Jr. *J. Mol. Spectrosc.* **1972**, *44*, 504.
- Carreira, L. A.; Mills, I. M.; Person, W. B. *J. Chem. Phys.* **1972**, *56*, 1444.
- Harthcock, M. A.; Laane, J. *J. Phys. Chem.* **1985**, *89*, 4231.
- Colegrove, L. F.; Wells, J. C.; Laane, J. *J. Chem. Phys.* **1990**, *93*, 6291.
- Choo, J.; Laane, J. *J. Chem. Phys.* **1994**, *101*, 2772.
- (a) Cortez, E.; Verastegui, R.; Villarreal, J.; Laane, J. *J. Am. Chem. Soc.* **1993**, *115*, 12312. (b) Choo, J.; Cortez, E.; Laane, J. *Proc. Int. Conf. FT-Spectrosc.* **1993**, *9*, 26.
- (a) Rivera-Gaines, V. E.; Leibowitz, S. J.; Laane, J. *J. Am. Chem. Soc.* **1991**, *113*, 9735. (b) Anet, F. A. L.; Freedberg, D. I.; Storer, J. W.; Houk, K. N. *J. Am. Chem. Soc.* **1992**, *114*, 10969. (c) Laane, J.; Choo, J. *J. Am. Chem. Soc.* **1994**, *116*, 3889.
- Choo, J.; Meinander, N.; Villarreal, J. R.; Laane, J. *J. Chem. Phys.* **1995**, *102*, 9506.
- Lord, R. C.; Rounds, T. C.; Ueda, T. *J. Chem. Phys.* **1972**, *57*, 2572.
- Wells, J. A.; Malloy, T. B. *J. Chem. Phys.* **1974**, *62*, 2132.
- Lopez, J. C.; Alonso, J. L. *Z. Naturforsch.* **1985**, *40a*, 913.
- Allinger, N. L.; Sprague, J. T. *J. Am. Chem. Soc.* **1972**, *94*, 5734.
- Anet, F. A. L.; Yavari, I. *Tetrahedron* **1978**, *34*, 2879.
- Dixon, E. A.; King, G. S. S.; Smithson, T. L.; Wieser, H. *J. Mol. Struct.* **1981**, *71*, 97.
- Tecklenburg, M. M. J.; Laane, J. *J. Mol. Spectrosc.* **1989**, *137*, 65.
- Tecklenburg, M. M. J.; Laane, J. *J. Am. Chem. Soc.* **1989**, *111*, 6920.
- Kilpatrick, E.; Pitzer, K. S.; Spitzer, R. *J. Am. Chem. Soc.* **1947**, *69*, 2183.
- Leibowitz, S. J.; Laane, J. *J. Chem. Phys.* **1994**, *101*, 2740.
- Laane, J. *In Vibrational Spectra and Structure*; Volume 1; Durig, J. R. Ed.; Dekker: New York, 1972.
- Burket, U.; Allinger, N. L. *Molecular Mechanics*; American Chemical Society Monograph; American Chemical Society; Washington, 1982.
- Choo, J.; Laane, J.; Majors, R.; Villarreal, J. R. *J. Am. Chem. Soc.* **1993**, *115*, 8396.

## Wholly Aromatic Polyesters Containing NLO Chromophores in the Side Chain

Suck-Hyun Lee, Ki-Cheon Lim, Jong-Taek Jeon, and Seog-Jeong Song\*

Department of Applied Chemistry, College of Engineering, Ajou University Suwon 442-749, Korea

\*Kolon Group Central Research Institute, Yongin-gun, Kyunggi-do 449-910, Korea

Received August 21, 1995

A series of poly(1,4-phenylene terephthalates) with pendant NLO chromophores was prepared by the solution polycondensation of 2,5-NLO chromophore substituted terephthalic acid with hydroquinone. The polymers obtained gave satisfactory NMR and elemental analysis results when taking into account their expected structures and the inherent viscosity value proved the polymeric character of all polymers. DSC, optical polarizing microscopy and WAXS studies revealed that none of these polymers exhibited liquid crystalline mesophases. Preliminary results on NLO properties of these polymers showed a surprisingly large second harmonic signal relative to a Y-cut quartz plate.

### Introduction

There has been a tremendous growth of interest in the field of nonlinear optical (NLO) polymers since polymeric materials offer the attractive combinations of optical, structural and processing properties. Among the NLO properties, second harmonic generation (SHG) is the first observed effect and has also been the most widely studied.<sup>1</sup> It is now well known that this frequency doubling activity requires

a stable non-centrosymmetric macroscopic structure and very few organic materials crystallize into nonsymmetric space groups. Various approaches with polymeric system to create noncentrosymmetric structures have been attempted.

Examples of polymeric materials exhibiting SHG include<sup>1</sup>:

- Guest-host polymer systems in which the active molecules are simply dissolved or distributed in the polymer matrix,
- Electro-optic polymers in which the active molecules are covalently bonded either to the polymer side chain or